Detecting Common Insulation Problems in Built Environments using Thermal Images

Naima Khan*, Nilavra Pathak*, Nirmalya Roy*
*Department of Information Systems, University of Maryland, Baltimore County nkhan4@umbc.edu, nilavra1@umbc.edu, nroy@umbc.edu

Abstract—Proper thermal insulation yields optimum energy expenses in buildings by maintaining necessary heat gain or loss through the built envelope. However, improper thermal insulation causes significant energy wastage along with infusing various damages on indoor and outdoor walls of the buildings, for example, damp areas, black stains, cracks, paint bubbles etc. Therefore, it is important to inspect the temperature variations in different areas of the built environments in regular basis. We propose a method for identifying temperature variance in building thermal images based on Symbolic Aggregated Approximation (SAX). Our process helps detect the temperature variation over different image segments and infers the fault prone segments of leakages. We collected about 50 thermal images associated with different types of wall specific insulation problems in indoor built environment and were able to identify the affected area with approximately 75% accuracy using our proposed method based on temperature variation detection approach.

Index Terms—Thermal Images, Building quality assessment, Symbolic Aggregated Approximation (SAX)

I. INTRODUCTION

Preventing wall surfaces from damages is an important concern as most homeowners spend approximately \$972 to \$2,722 for interior wall designs and on an average of \$670 for every repair, excluding the cost of hiring contractors [1], [2]. Besides energy efficiency, good thermal insulation helps to maintain thermal comfort for the occupants, prevents severe wall damages by controlling moisture in the wall surfaces [3], [4]. Thermal insulation governs the heat flow from and to the buildings and is primarily determined by the materials used for construction [5]. Moreover, damp inside the building causes change in relative humidity thus changing indoor environment due to its correlation with temperature [6]. Building inspectors use handheld thermal cameras or infrared thermography to identify the defects in the built environment. Surface temperature alone can explain 80% of the observed variation in air temperature [7]. Researchers analyze the temperature profile of a building both from indoors and the outdoors with thermal camera. Qualitative visual analysis of outer building surface with thermal images reveal the defective areas in energy audits [8], [9]. Blower door tests by pressurizing homes along with thermal imaging help detect leakages in buildings [10] which requires expert assistance and causes recurring costs. Using thermal camera is preferable to other intrusive methods and a fixed cost way to check around the temperature differences occurring inside and outside of the buildings. Thermal camera highlights the hotter and cooler regions in the thermal images with different palettes, but that's not sufficient to infer the location of temperature discords or the thermal characteristics of leakages from the original thermal images. Besides interpret ability issues with thermal images were reported in [11]. Though qualitative analysis with temperature of building envelop has been done in literature, there is still lack of easily applicable quantitative temperature analysis of leakages.

Motivated by the previous works, we conducted a study to assess the thermal images of the indoor built environments and determined a systematic approach for extracting leakage areas from the collected data. To process the building thermal images, we segmented the image areas based on temperature with different existing image segmentation algorithms. Not all segmentation algorithms provide satisfactory temperature segmentation with effective execution time. We applied three different kinds of segmentation algorithms i.e. simple linear iterative clustering (SLIC), gradient ascent based Watershed and graphical hierarchical clustering based Felzenswalb, to generate superpixels based on the temperature values of the pixels in the thermal image. To detect the temperature variation occurring locations in the image we used Symbolic Aggregate Approximation (SAX) [12] to represent the pixel temperature data of each segments. We propose SAX as it has been used to detect the unusual shapes in the images in [13]. In this paper, we introduced a systematic approach for detecting leakages from thermal images by proposing a SAX based technique to find temperature variations among the regions and identify wall segments in the image that have poor insulation. We detected the locations where temperature variation differs from the other places in the image. We showed that only temperature analysis from the thermal images can provide us an intuition of the affected or to be affected area in the inside wall.

The remaining paper is organized as follows. In Section II, we presented the relevant works related to our research. In Section III, we discussed our overall framework with detailed explanation for every step. In Section IV, we presented some of the experimental results. In Section V, we discussed our future research direction and finally we conclude in Section VI.

II. RELATED WORKS

Temperature analysis from inside and outside of the buildings with thermal images has been one research direction of non invasive building envelop monitoring. Recent researches [14] investigated the temperature variation inside



and outside of the buildings with thermal images along with the usability issues [15]. A qualitative analysis with image differences over time has been done with outside thermal images of the buildings built from last century in England [8] to detect the defected and shadowed areas in the outer envelop. Research in detecting air leakage and defects identification are concentrated in two major directions - parametric modeling of building insulation [16] and leakage detection [17]. While there is a significant research on thermal imaging for energy usage and leakage detection most of them utilize very high resolution (480 \times 360) thermal cameras that are extremely expensive. For example, using a thermal camera that cost upward of \$ 20000 ([18], [19]) will incur far higher startup cost and than saving power consumption. Motivated by these challenges we proposed IRLeak [20] in our previous research, a low cost low power thermal imaging unit that is capable of continuously capturing thermal data and conducted some preliminary analysis to detect energy leakage in homes. Due to the extreme low resolution of thermal camera (16×4), the data collection becomes particularly challenging. To identify the shortcomings of the low power camera, we conduct a systematic study with a moderately higher thermal resolution (80×60) to determine the feasibility of the second version of IRLeak. We initiated an approach to get an intuition of temperature variation through wall damages from one shot thermal images without other knowledge of the building parameters.

III. OVERALL FRAMEWORK

We present the overall framework for detecting defects in indoor built environments in Figure 1 and describe each of the blocks in details in the following sub-sections.

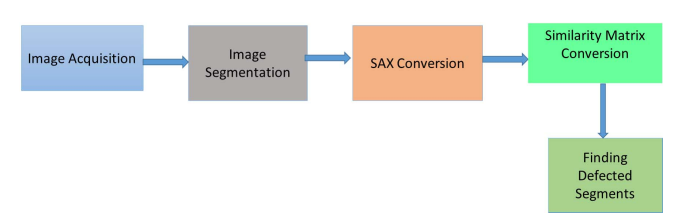
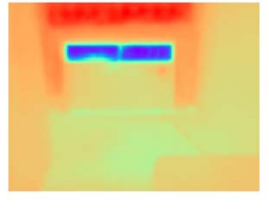


Fig. 1: Overall Framework

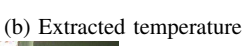
A. Image Acquisition

FLIROne camera combines both thermal and visual images together using Multi-Spectral Dynamic Imaging (MSX) technology. We extracted the temperature from thermal images using a R library named as Thermimage [21]. The extracted thermal images contain only temperature values for each of the pixels. In Figure 2, we show an example of the visual and thermal image captured using FLIROne camera, where the thermal image is constructed by mapping the temperature data in a RGB color domain.





(a) Original FLIROne Image





(c) Visual Image

Fig. 2: Thermal and Visual Image Extraction

B. Image Segmentation

In the second step, to determine regions with similar thermal characteristics we applied image segmentation. We compared three image segmentation algorithms,- Watershed [22], SLIC [23] and Felzenswalb [24], for dividing the thermal images into regions with similar temperature profiles. Our objective is to group the pixels in the thermal image into superpixels based on temperature values and each group is assigned with different segment numbers such that the images with similar temperature distributions are grouped together. We did not use any edge detection based segmentation algorithm as we are mostly interested in temperature values of the image rather than objects recognition in the image. Watershed algorithm divides the surface of temperature values from the thermal image, into some areas where the temperature is about to have a high or low peak. SLIC follows a similar idea of k-means clustering and finds the k-centers and assigns each pixels to the nearest center based on the difference of temperature between them. Felzenswalb performs a bottom up clustering of pixel nodes on a graph, such that each segment, the shortest spanning tree of the constituent pixels. However, for each segments, corresponding temperature series has been extracted. One temperature series represents the temperature for the pixels of corresponding segment.

C. Symbolic Aggregated Approximation (SAX) Conversion

In the next step we used Symbolic Aggregate approximation (SAX) [12] to transform temperature series of each segment into a string of alphabets. The SAX words compress the time series and reduce the execution time for computing comparison with other temperature series. SAX transforms a given time-series T of length n into a string of arbitrary length m (given), where $m \leq n$, using an alphabet A of size $a \geq 2$. As a prior step to applying SAX on the temperature data from thermal images, we standardized the time-series data by z-

normalization. The normalized time series T is converted to a vector of letters $X = (x_1, x_2, ..., x_m)$ of length $m \le n$, where

$$x_{i} = \frac{m}{n} \sum_{j=n/m(i-1)+1}^{(n/m)i} x_{j}$$
 (1)

We showed the SAX conversion of a series with an example in Figure 3. The temperature series of 100 points are divided into 10 parts (randomly chosen) and presented with alphabet size 10 by four cut-points to describe 10 parts with the letters from alphabet. Finally, SAX word for the series is 'iggiihebaa'.

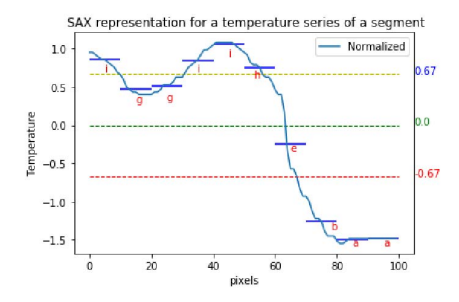


Fig. 3: SAX representation of temperature series

D. Constructing Similarity Matrix

We constructed a similarity matrix by comparing every pair of SAX words following the process described in [13]. Here we considered all the circular shifts of each SAX words to cover rotational invariance of temperature series. We checked if any of the circular shifts of one SAX word matches with the circular shifts of another SAX word. We created a sparse matrix M as similarity matrix to store the number of matches found for each of temperature series. The values in the similarity matrix denotes the number of matches found in SAX words of different masked lengths for each pair of the temperature series. Figure 4(a) shows the steps for constructing similarity matrix and figure 4(b) shows the similarity matrix among three series. Shaded columns in SAX words indicates those columns were hidden and circular shifts were done on the remaining characters from the SAX words. The columns and the number of columns to be hidden were chosen randomly. Similarity matrix showed series T_1 and T_2 has two matches in this iteration and T_3 has no match with the others.

E. Finding Defected Segments

After constructing the similarity matrix we extracted the list of temperature series which have no match with other temperature series. We calculated euclidean distance among these series and make a list of nearest neighbor distance for each of them. Empirically we determined the defected segments have higher nearest neighbor distance than the half of the maximum distance of the list. Finally we highlighted the defected segments with different colored boxes.

In the algorithm 1 we have formally presented our proposed method.

Algorithm 1 Finding Leakage Segments

- 1: **procedure** TEMPERATURE VARIATION(Image *I*)
- 2: T = ExtractThermalImage(I)
- 3: $S \leftarrow Segmentation(T)$ \triangleright Image Segmentation
- 4: $TempSeries \leftarrow ExtractTemperature(S)$
- 5: $SAXwords \leftarrow SAX(TempSeries) \rightarrow SAX$ conversion
- 6: M ← Match() > Match function returns number of matches found among SAXwords following process showed in Figure 4
- NonMatchSeg ← M_i if M_i == 0 ▷ List of temperature series with no matches found
- 8: NNDist ← NearestNeighborDistance(NonMatchSeg)

 ▷ List of nearest neighbor distances for segments in

 NonMatchSeg
- 9: MaxNNDist ← Max(NNDist) > Maximum distance among nearest neighbor distances
- 10: $DefectedSegments \leftarrow S_i \text{ if } NNDist_i \geq MaxNNDist/2$
- 11: **return** DefectedSegments

IV. EXPERIMENTAL RESULTS

In this section we will demonstrate how our method works for a thermal image as well as present the performance for our method.

A. Data collection

We collected 50 thermal images from a variety of wall surfaces with different quality of insulation with a FLIROne camera and Android smartphone. We collected thermal images of different affected places in 9 different rooms from inside and outside of the buildings. Our thermal images cover moisture problems, insulation problems around the window area, cracks, electric outlet holes, thermal bridging, paint bubbles, damp areas. For our data collection we used Samsung Galaxy S6 which has the screen size of 5.1 inches. Our thermal image resolution is 640×480 or vice versa.

B. Extracting thermal images

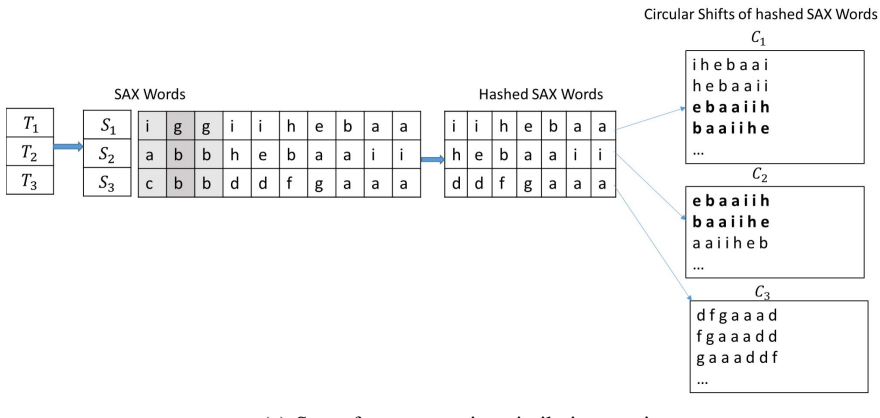
Temperature information was extracted from the thermal image using Plank's law and the Stephan Boltzmann relationship, as well as atmospheric absorption, camera IR absorption, emissivity. The temperature extraction from the thermal image is implemented in a R package named Therimage [21]. Extracted thermal image contains only temperature values for each of pixels.

C. Analysis of Thermal Image Segmentation

We applied the three image segmentation algorithms – watershed, slic and felzenswalb on each thermal images. Figure 5 depicts segmentation of the thermal images using these algorithms. We obtained three segments with slic, five segments with watershed as well as six segments with felzenswalb.

D. SAX and discord detection

After segmenting the thermal images, we converted each of the segment's temperature series into SAX word. Then we identified the segments as defected for which no match was found and their nearest neighbor distance is higher than of the



(a) Steps for constructing similarity matrix

	T_1	T_2	T_3
T_1		2	0
T_2	2		0
T_3	0	0	

(b) Similarity Matrix

Fig. 4: Steps for constructing Similarity Matrix

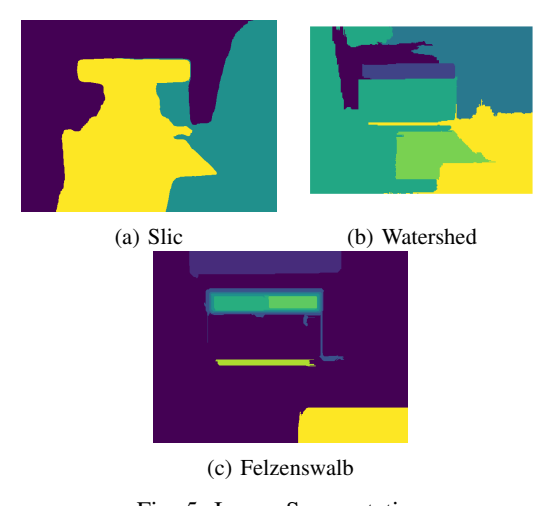


Fig. 5: Image Segmentation





(a) Defected segments with (b) Defected segments with Slic Watershed



(c) Defected segments with Felzenswalb

Fig. 6: Defected Segments with three segmentation algorithms

others. We constructed similarity matrix for the temperature series obtained from all of three segmentation algorithms. Figure 6 shows the discord segments obtained from the three segmentation algorithms and SAX. This figure shows the defected segments with bounding box and the segment number is written in the center of the box. It seems window with air condition is identified as defected in all of the three figures in figure 6. We manually annotated the visible leakage area and calculated pixel wise evaluation metrics for the obtained pixels of the defected segments. We defined the evaluation metrics as follows:

$$Accuracy = \frac{\text{\# of identified defected pixels}}{\text{Total \# of defected pixels}}$$
 (2)

$$Precision = \frac{\text{\# of correctly identified defected pixels}}{\text{\# of predicted defected pixels}} \quad (3)$$

$$Recall = \frac{\text{# of correctly identified defected pixels}}{\text{# of actual defected pixels}}$$
 (4)

Table I shows the accuracy, precision, recall and execution time for our proposed method using three different types of superpixel construction i.e. watershed, slic and felzenswalb. Felzenswalb took almost 1 minute to execute for a single thermal image.

Methods	Accuracy	Precision	Recall	Avg. Execution Time
Slic	75.54%	66.85%	89.79%	32.45s
Watershed	69.6%	79.72%	65.60%	44.45s
Felzenswalb	57.06%	41.89%	50.0%	58.07s

TABLE I: Evaluation of defect detection with SAX on different segmentation techniques

From the evaluation metrics, it appears that slic segmentation provides better accuracy in defect detection while watershed segmentation provides better precision. Felzenswalb segmentation performs poorly and couldn't detect any segments as defected for 9 images out of 50 images.

V. FUTURE WORKS

Longitudinal thermal image acquisition with smartphone is a big challenges due to deployment, privacy and battery charge issues. Therefore, we propose to construct a new thermal imaging edge device that improves our prior IRLeak [20] unit where we propose to use the FIIR devkit that consists of an 80 × 60 thermal camera controlled by a Raspberry Pi Zero. In the previous unit we constructed the unit using an MLX90621 IR camera unit that has a very low resolution of 16 × 4 thermal imaging pixels. Also, the field of view of the camera was very limited, therefore it was required to be placed on top of a stepper motor that rotated the whole system with precision movements. Now we propose to use a Raspberry Pi 3, unlike the Pi Zero used in the previous system, for utilizing the onboard GPU to speed up computation particularly when we plan to deploy deep neural networks. In the future, we will focus on studying the longitudinal effects of leakage by continuously monitoring the indoor environment with our proposed system.

VI. CONCLUSION

In this study we explored the thermal characteristics of a building insulation using a commercially available thermal camera. We proposed a systematic approach to detect the defective areas in the blue building walls based on temperature variance. We found that the segments that have poor insulation or damages have higher variance in temperature. In this work, we introduced an approach to determine the temperature variation of the leakage or damaged areas in the built environments which can be used by the end user for regular evaluation.

VII. ACKNOWLEDGMENT

This work is supported by the NSF CNS grant 1544687.

REFERENCES

- "2018 wall and ceiling costs average cost to build an interior wall," 2018.
- [2] "2018 wall repair costs fix holes, cracks, bowed walls and more homeadvisor," 2018.
- [3] C. D. Korkas, S. Baldi, I. Michailidis, and E. B. Kosmatopoulos, "Occupancy-based demand response and thermal comfort optimization in microgrids with renewable energy sources and energy storage," *Applied Energy*, vol. 163, pp. 93–104, 2016.

- [4] H. B. Rijal, M. A. Humphreys, and J. F. Nicol, "Development of a window opening algorithm based on adaptive thermal comfort to predict occupant behavior in japanese dwellings," *Japan Architectural Review*, vol. 1, no. 3, pp. 310–321, 2018.
 [5] U. Berardi, "The impact of temperature dependency of the building in-
- [5] U. Berardi, "The impact of temperature dependency of the building insulation thermal conductivity in the canadian climate," *Energy Procedia*, vol. 132, pp. 237–242, 2017.
- [6] J. L. Nguyen, J. Schwartz, and D. W. Dockery, "The relationship between indoor and outdoor temperature, apparent temperature, relative humidity, and absolute humidity," *Indoor air*, vol. 24, no. 1, pp. 103– 112, 2014
- [7] S. Kawashima, T. Ishida, M. Minomura, and T. Miwa, "Relations between surface temperature and air temperature on a local scale during winter nights," *Journal of Applied Meteorology*, vol. 39, no. 9, pp. 1570– 1579, 2000.
- [8] M. Fox, D. Coley, S. Goodhew, and P. De Wilde, "Time-lapse ther-mography for building defect detection," *Energy and Buildings*, vol. 92, pp. 95–106, 2015.
- [9] M. L. Mauriello and J. E. Froehlich, "Towards automated thermal profiling of buildings at scale using unmanned aerial vehicles and 3dreconstruction," in *Proceedings of the 2014 ACM International Joint Conference on Pervasive and Ubiquitous Computing: Adjunct Publica*tion, pp. 119–122, ACM, 2014.
- [10] E. Barreira, R. M. Almeida, and M. Moreira, "An infrared thermography passive approach to assess the effect of leakage points in buildings," *Energy and Buildings*, vol. 140, pp. 224–235, 2017.
- [11] M. L. Mauriello, L. Norooz, and J. E. Froehlich, "Understanding the role of thermography in energy auditing: current practices and the potential for automated solutions," in *Proceedings of the 33rd Annual ACM* Conference on Human Factors in Computing Systems, pp. 1993–2002, ACM, 2015.
- [12] J. Lin, E. Keogh, S. Lonardi, and B. Chiu, "A symbolic representation of time series, with implications for streaming algorithms," in *Proceedings* of the 8th ACM SIGMOD workshop on Research issues in data mining and knowledge discovery, pp. 2–11, ACM, 2003.
- [13] L. Wei, E. Keogh, X. Xi, and M. Yoder, "Efficiently finding unusual shapes in large image databases," *Data Mining and Knowledge Discov*ery, vol. 17, no. 3, pp. 343–376, 2008.
- [14] M. L. Mauriello, "Scalable methods and tools to support thermographic data collection and analysis for energy audits," in *Proceedings of the* 2017 ACM International Joint Conference on Pervasive and Ubiquitous Computing and Proceedings of the 2017 ACM International Symposium on Wearable Computers, pp. 360–364, ACM, 2017.
- [15] M. L. Mauriello, J. Chazan, J. Gilkeson, and J. E. Froehlich, "A temporal thermography system for supporting longitudinal building energy audits," 2017.
- [16] P. Bacher and H. Madsen, "Identifying suitable models for the heat dynamics of buildings," *Energy and Buildings*, vol. 43, no. 7, pp. 1511– 1522, 2011.
- [17] M. H. Sherman, "Superposition in infiltration modeling," *Indoor Air*, vol. 2, no. 2, pp. 101–114, 1992.
- [18] B.-J. Ho, H.-L. C. Kao, N.-C. Chen, C.-W. You, H.-H. Chu, and M.-S. Chen, "Heatprobe: a thermal-based power meter for accounting disaggregated electricity usage," in *Proceedings of the 13th international* conference on Ubiquitous computing, pp. 55–64, ACM, 2011.
- [19] W. Liu, X. Zhao, and Q. Chen, "A novel method for measuring air infiltration rate in buildings," *Energy and Buildings*, vol. 168, pp. 309– 318, 2018.
- [20] D. Lachut, N. Pathak, N. Banerjee, N. Roy, and R. Robucci, "Longitudinal energy waste detection with visualization," in *Proceedings of the 4th ACM International Conference on Systems for Energy-Efficient Built Environments*, BuildSys '17, (New York, NY, USA), pp. 7:1–7:4, ACM, 2017
- [21] G. J. Tattersall, "Thermimage: Thermal image analysis," Dec. 2017.
- [22] R. C. Gonzalez, R. E. Woods, et al., "Digital image processing," 2002.
- [23] R. Achanta, A. Shaji, K. Smith, A. Lucchi, P. Fua, S. Süsstrunk, et al., "Slic superpixels compared to state-of-the-art superpixel methods," *IEEE transactions on pattern analysis and machine intelligence*, vol. 34, no. 11, pp. 2274–2282, 2012.
- [24] P. F. Felzenszwalb and D. P. Huttenlocher, "Efficient graph-based image segmentation," *International journal of computer vision*, vol. 59, no. 2, pp. 167–181, 2004.